Computational and Experimental Investigation of Alkene Hydrogenation by a Pincer-Type [P_2Si]Rh Complex: Alkane Release via Competitive σ-Bond Metathesis and Reductive Elimination

Matthew T. Whited,*,† Michael J. Trenerry,†,§ Kaitlyn E. DeMeulenaere,†,§ and Buck L. H. Taylor,*,†,‡

† Department of Chemistry, Carleton College, Northfield, MN 55057, United States

‡ Department of Chemistry, University of Portland, Portland, OR 97203, United States

ABSTRACT: A combined experimental and computational approach has been utilized to elucidate the mechanism of alkene hydrogenation by pincer-type [P_2Si]Rh catalysts. Although [P_2Si]Rh interacts with H_2 to afford a dihydrogen σ-complex rather than a dihydride (seemingly an indication of facile reductive elimination from Rh(III)), alkane release occurs by competitive σ-bond metathesis (bimolecular) and reductive elimination (unimolecular) pathways. This unusual behavior is attributed to the strong *trans* influence of the silyl donor.

INTRODUCTION

Alkene hydrogenation is one of the most widely utilized and best studied metal-catalyzed transformations. The importance of the hydrogenation reaction has prompted numerous experimental and computational mechanistic studies on a variety of effective catalysts in order to understand factors influencing rate and selectivity.[1]

Broadly speaking, hydrogenation catalysts can be separated into two classes based on the mechanisms of H_2 activation and alkane release. Early-metal and lanthanide catalysts, which are frequently found in their highest oxidation states, typically activate H_2 and release alkane by σ-bond metathesis.[2] A σ-bond metathesis pathway is also often followed by Ru catalysts,[3] with the distinction that H_2 σ-adduct intermediates may precede hydrogen transfer and the intimate mechanism has thus been denoted σ-complex-assisted metathesis, or σ-CAM.[4] Alternatively, the ubiquitous catalysts based on Rh and Ir normally activate H_2 by oxidative addition and release alkane by reductive elimination.[5] To our knowledge, there has been no study showing competing alkane release mechanisms for late metals.

As part of a research program aimed at developing new approaches to metal/silicon cooperative small-molecule activation,[6] we recently reported a triflatosilyl [$^{Cy}P_2Si^{OTf}$]Rh pincer-type complex that can activate H_2 across the Rh–Si bond, subsequently delivering the H_2 unit to a strained alkene (Scheme 1).[7] Although the complex is active for catalytic norbornene (nbe) hydrogenation, comparative studies against a related methylsilyl [$^{Cy}P_2Si^{Me}$]Rh complex that cannot activate H_2 in the same fashion indicated that Rh/Si cooperation is not required for catalysis. On the contrary, the triflatosilyl complex is a considerably less efficient hydrogenation catalyst than its methylsilyl analogue. Based on these findings, we proposed the mechanism displayed in Figure 1. The proposed cycle accounts for the relatively lower efficiency of triflatosilyl catalysts relative to methylsilyl catalysts, which may be related to the equilibrium that siphons active catalyst away from the cycle.

Scheme 1. H_2 activation across a Rh–Si bond at [$^{Cy}P_2Si^{OTf}$]Rh[7]

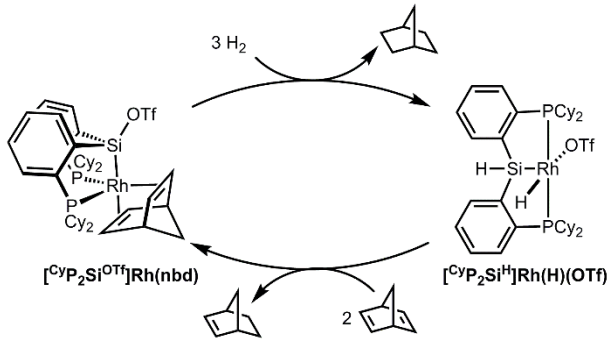

Nevertheless, Figure 1 indicates that several important unanswered questions remain regarding hydrogenation by pincer-type [P_2Si]Rh complexes. First, what is the nature of the RhH_2 species? Earlier calculations suggested a σ-complex of H_2,[7] but at the time we had no experimental support for the finding and were unsure how alkene insertion could occur at such an intermediate. Second, what is the mechanism of alkane release? Unimolecular reductive elimination from a norbornyl hydride complex (Path A in Figure 1) would be the most obvious route based on precedent. However, formation of significant amounts of norbornane-d_1 (nba-d_1) under H_2/D_2 suggested that alkane release from a norbornyl hydride (or isomer) could be a bimolecular process involving a second molecule of H_2 or D_2 (Path B in Figure 1).

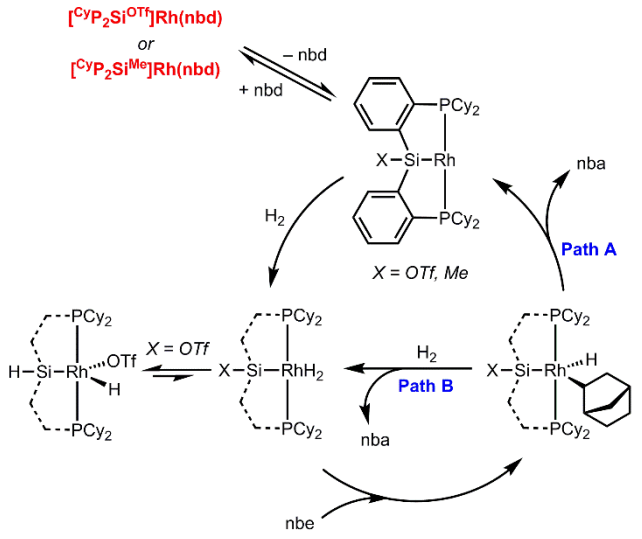

Figure 1. Previously proposed cycle for alkene hydrogenation by [P$_2$Si]Rh complexes (nbe = norbornene, nba = norbornane)[7]

Herein we address the above questions through a combined computational and experimental investigation of nbe hydrogenation by methylsilyl [P$_2$Si^{Me}]Rh pincer-type complexes. In the first part of this paper, we use density functional theory (DFT) to elucidate the intimate mechanism(s) of nbe hydrogenation by [P$_2$Si^{Me}]Rh, leading to two important findings: 1) the reaction of H$_2$ with the hydrogenation catalyst may afford either η^2-H$_2$ or dihydride complexes, for which energies are computed to be quite similar, and 2) reductive elimination (unimolecular) and σ-bond metathesis (bimolecular) are both energetically viable pathways for alkane release. In the second part of this paper, we provide experimental observations elucidating the computations, identifying a stable dihydrogen adduct of [^{Cy}P$_2$Si^{Me}]Rh and using isotopically labeled hydrogen to demonstrate competitive uni- and bimolecular alkane release pathways (Paths A and B in Figure 1) that can be tuned by changing temperature and hydrogen concentration. Together, these findings provide a unified view of the unusual mechanistic regime accessed as a consequence of the strongly *trans*-influencing central silyl donor.

RESULTS AND DISCUSSION

Computational Studies of Alkene Hydrogenation by [P$_2$Si]Rh. Computational studies were performed using density functional theory (DFT) on model catalyst [^{Me}P$_2$Si^{Me}]Rh (**1**), in which the cyclohexyl groups are truncated to methyl and norbornadiene has dissociated (Figure 2). Calculations were performed in Gaussian 09.[8] We selected a theoretical method based on a benchmark study of alkene hydrogenation with a ruthenium Xantphos catalyst.[1f] The B97-D3BJ density functional was used with the def2-TZVP basis set and IEF-PCM model for diethyl ether. Thermal corrections were calculated at room temperature (298 K) and an elevated pressure (235 atm) to account for entropy effects in solution. This theoretical method reproduced experimental free energy spans with deviations of about 1 kcal/mol in Leitner's benchmark study.[1f] Other theoretical methods are evaluated in the Supporting Information.

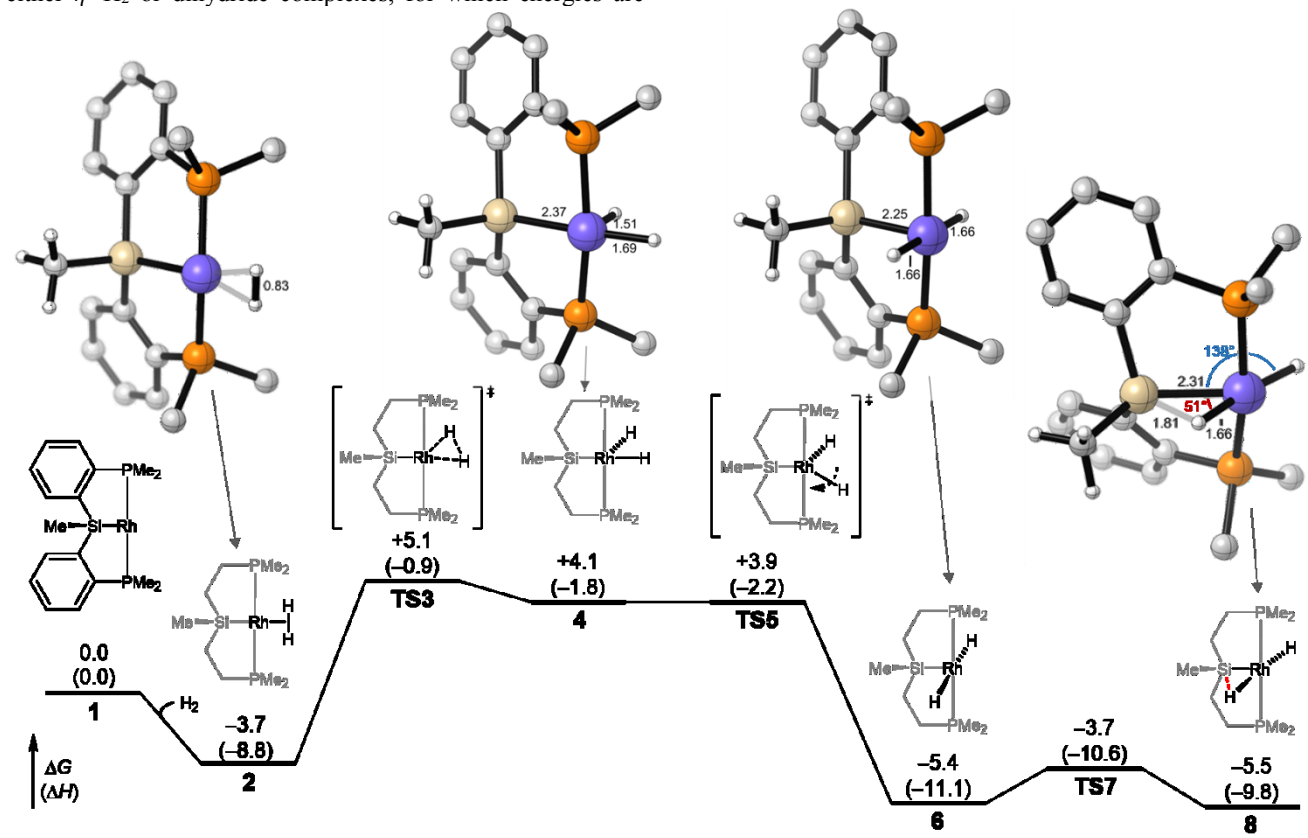

Figure 2. Reaction pathway of model catalyst **1** with H$_2$ in the absence of alkene. Gibbs free energies and enthalpies (in parentheses) calculated with B97-D3BJ/def2-TZVP/IEF-PCM(diethyl ether).

First, the reaction of model catalyst **1** with H_2 in the absence of alkene was modeled to compare to later experimental observations (Figure 2). Binding of H_2 is weakly exergonic and forms square-planar σ-complex **2** in which the H_2 molecule is oriented along the square plane (vertical in Figure 2), and the H–H bond is elongated by about 0.1 Å (to 0.83 Å). Oxidative addition requires rotation of H_2 (horizontal in Figure 2), which is not a stable structure, but costs about 1 kcal/mol. Oxidative addition via **TS3** gives dihydride complex **4**, in which the hydrides occupy sites *trans* to the silicon and *anti* to the Si–Me bond. We are unable to locate a diastereomeric transition state that would lead to a hydride *syn* to the Si–Me bond.

Other isomers of dihydride **4** have been explored. Isomerization via **TS5** occurs with essentially no barrier ($\Delta E^{\ddagger}$ = 0.6 kcal/mol from **4**) to *trans*-dihydride **6**, which has a square pyramidal geometry. We are unable to locate a *cis*-dihydride complex in which one hydride is *syn* to the Si–Me bond. Instead, rearrangement of the hydride ligands gives complex **8**, which has a Y-type geometry with an acute Si–Rh–H angle (51°), while maintaining a nearly *trans* orientation of the hydride ligands (171°). There is clearly a modest bonding Si–H interaction (1.81 Å; typical Si–H bond length = 1.48 Å) around the cutoff between η^2-SiH and a secondary interaction (SISHA).[9] Further calculations indicate that neither **6** nor **8** is capable of binding to nbe, which dissociates during geometry optimization. We therefore conclude that **6** and **8** are not relevant to the hydrogenation mechanism but may be in equilibrium with the dihydrogen complex **2**.

Dihydride complex **4** is also capable of binding a second molecule of H_2 leading to σ complex **9** (Figure 3). σ-bond metathesis (**TS10**) can occur with a low barrier to afford isomeric complex **11**, which is in equilibrium with dihydride **6**. This pathway would allow rapid H/D scrambling if isotopically labelled hydrogen were employed ($\Delta G^{\ddagger}$ = 11.9 kcal/mol from **11** to **4**). However, such scrambling may be significantly inhibited in the presence of alkene (*vide infra*).

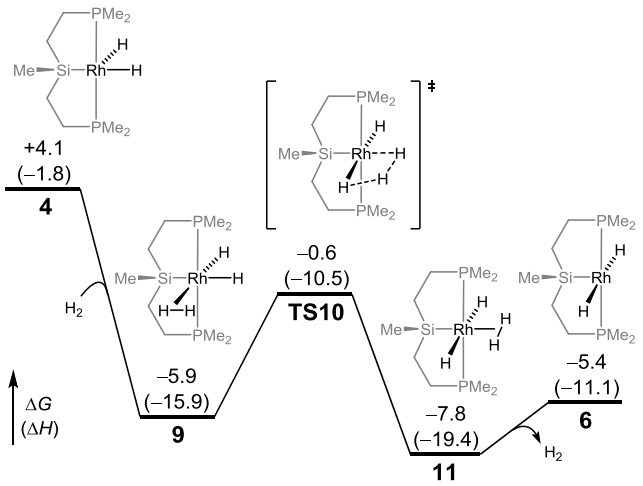

Figure 3. Reaction pathway of model catalyst **1** with H_2 in the absence of alkene. Gibbs free energies and enthalpies (in parentheses) in kcal/mol, with respect to the alkene catalyst **1**.

We next studied the activation of H_2 in the presence of alkene (Figure 4). Binding of nbe to model catalyst **1** is very exergonic, forming complex **12**, which is the resting state on the catalytic cycle; all energies in Figure 4 and later figures are computed with respect to **12**. There is a preference for binding nbe from the *exo* face, which persists throughout the hydrogenation pathway. Hydrogen binding is endothermic, forming a relatively unstable η^2-H_2 complex **13**, with a roughly trigonal bipyramidal geometry. We have located a transition state for H_2-binding, which is iso-energetic with σ-complex **13** and is therefore omitted from Figure 4 (see Supporting Information). Splitting of H_2 via oxidative addition (**TS14**) forms octahedral dihydride **15** with essentially no barrier. Importantly, alkene binding stabilizes dihydride complex **15** relative to η^2-H_2 complex **13** and results in a lower-energy transition state for oxidative addition of H_2. Norbornene complex **15** undergoes facile migratory insertion via **TS16** to give alkyl complex **17**.

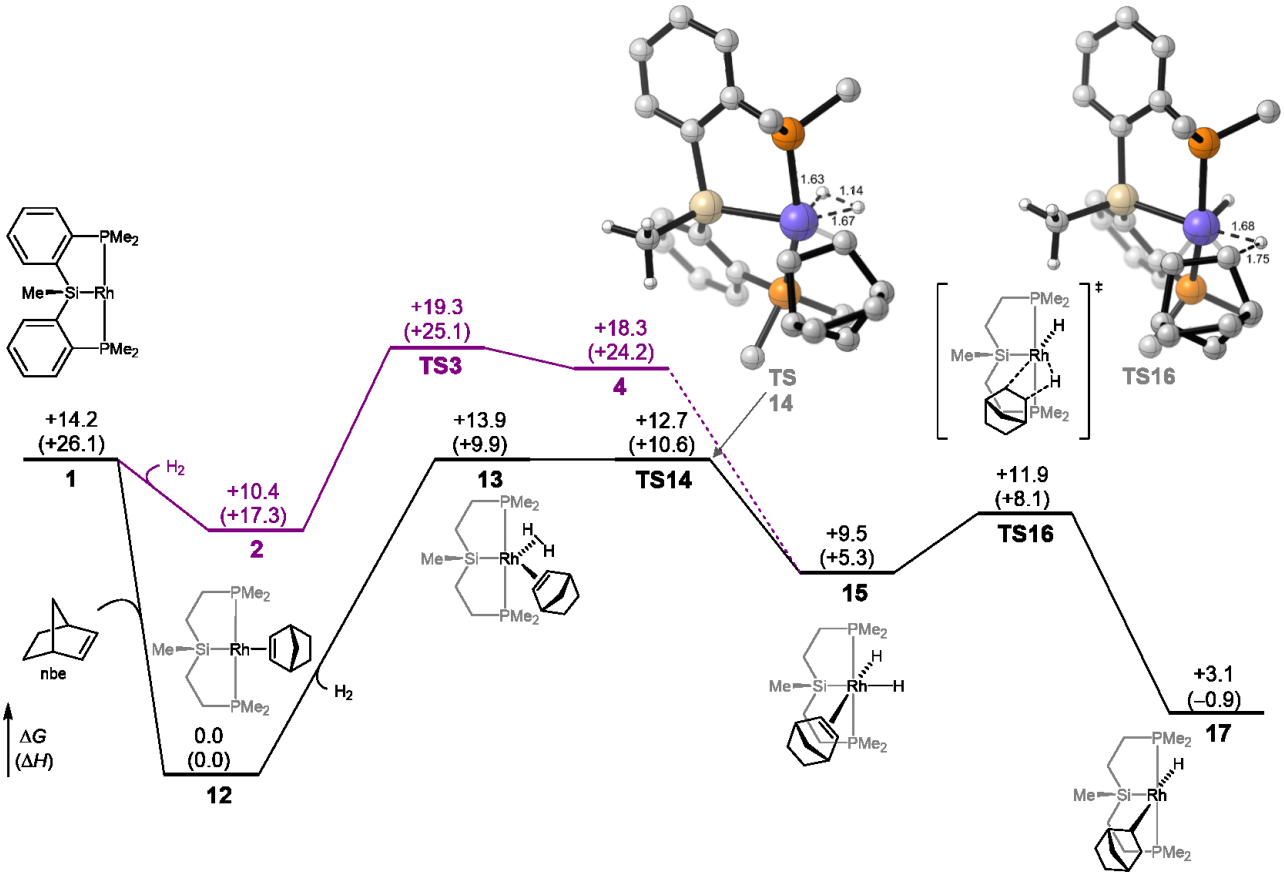

Figure 4. Activation of H_2 by model catalyst **1** in the presence (black) and absence (purple) of alkene. Gibbs free energies and enthalpies (in parentheses) in kcal/mol, with respect to the alkene complex **12**.

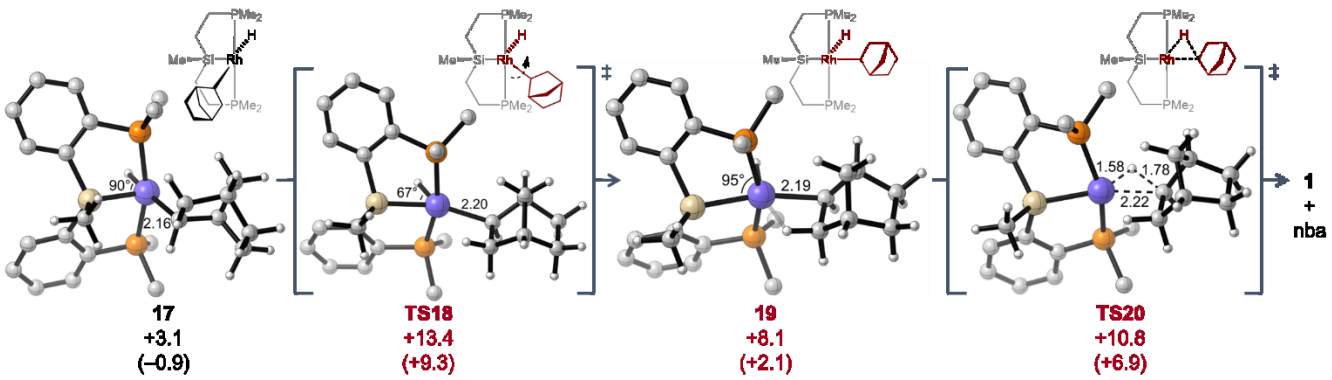

Figure 5. Unimolecular mechanism for alkane release, including isomerization of the norbornyl ligand and reductive elimination. Gibbs free energies and enthalpies (in parentheses) in kcal/mol, with respect to the alkene complex **12**.

Complex **17** initially has hydride and norbornyl ligands in a *trans* orientation (Figure 5), due in part to the greater *trans* influence of the silyl versus norbornyl and hydride ligands.[10] In order for unimolecular alkane release to occur, the norbornyl ligand must isomerize via **TS18** to **19**. There is a preference for norbornyl migration over hydride migration, again a probable consequence of relative *trans* influences (H > R). Both **17** and **19** are approximately square pyramidal with a Si–Rh–H bond angle near 90°. **TS18** features a Y-type geometry with a Si–Rh–H bond angle of 67°. During this step, the hydride initially moves toward the silicon atom, then back to its original position, indicating a preference to remain *trans* to the norbornyl ligand; a similar phenomenon occurs during hydride isomerization in **TS5** (Figure 2). An intrinsic reaction coordinate (IRC) calculation confirms that **TS18** links **17** and **19** without an additional intermediate (see Supporting Information). Complex **19** undergoes facile reductive elimination (**TS20**) to release nba and regenerate catalyst **1**.

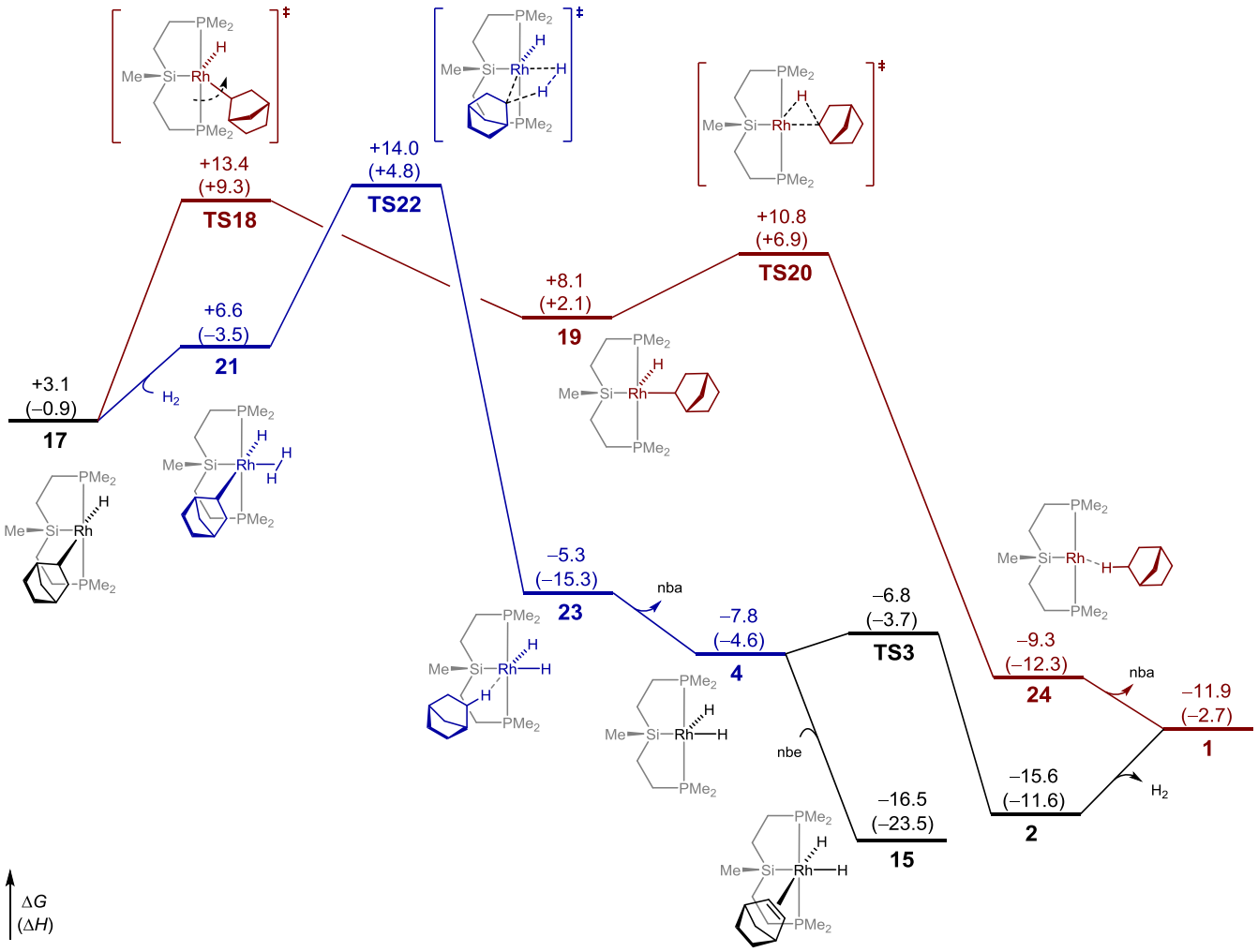

Figure 6. Formation of alkane via bimolecular (blue) and unimolecular (red) pathways. Gibbs free energies and enthalpies (in parentheses) in kcal/mol, with respect to the alkene complex **12**.

The initial alkyl complex **17** is also capable of a bimolecular mechanism for alkane release (Figure 6, blue pathway). The bimolecular pathway proceeds by binding an additional molecule of H_2 to afford σ-complex **21**. The transition state for H_2-binding is again very similar in energy to **21** (Supporting Information). An isomer of **21** in which H_2 is *trans* to norbornyl is significantly higher in energy, likely a consequence of the high relative trans influence of the silyl ligand (Figure S5). Complex **21** then undergoes σ-bond metathesis via **TS22** to afford nba σ-complex **23**. The fact that a σ-adduct intermediate precedes σ-bond metathesis indicates that the process is best denoted as σ-CAM, and the kite-shaped geometry of **TS22** is consistent with previous reports of σ-CAM.[4] Finally, release of nba forms dihydride **4**, which may either bind nbe to form **15** (continuing the catalytic cycle) or release H_2 to regenerate catalyst **1**.

The unimolecular (red) and bimolecular (blue) mechanisms for alkane release are calculated to be very similar in free energy with our chosen model system ($\Delta\Delta G^{\ddagger}$ = 0.6 kcal/mol). To confirm that this is a valid conclusion for the full catalyst we recalculated key transition states for alkane release using full cyclohexyl substituents on the phosphine ligands (Figure 7). Due to the size of this system, geometries were optimized using a smaller basis set (def2-SVP) and single-point energies were calculated with our standard basis set (def2-TZVP). The barriers, with respect to alkene complex **12-Cy**, are about 17 kcal/mol (3 kcal/mol higher than the truncated model). Importantly, the relative barriers for unimolecular (**TS18-Cy**) and bimolecular (**TS22-Cy**) alkane release are identical to the model system: reductive elimination is favored by 0.6 kcal/mol.

Thus, with both the truncated and full models, the barriers for σ-bond metathesis and reductive elimination pathways are very close. The bimolecular mechanism is enthalpically favored but entropically disfavored. Therefore, the free energy difference between the two pathways depends greatly on how entropy is calculated in solution, for which there is significant uncertainty. Here an elevated pressure (235 atm or 9.6 mol/L) is specified to account for entropy effects in solution,[1f] but other treatments are shown in the Supporting Information. For example, at a standard state of 1.0 mol/L, the unimolecular pathway is favored by 2.0 kcal/mol. Rather than predict an exact preference, we conclude from computation that the two mechanisms may be competitive under typical conditions and that the ratio between the two mechanisms will depend on parameters that affect entropy (temperature and H_2 pressure).

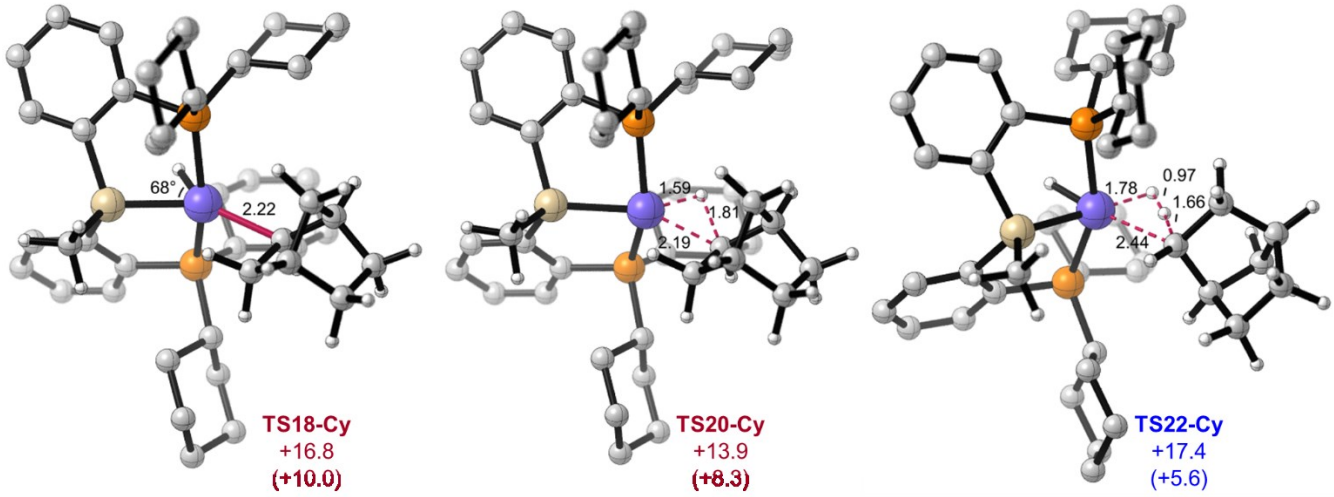

Figure 7. Key transition states with full dicyclohexylphosphine ligand. Gibbs free energies and enthalpies (in parentheses) in kcal/mol, with respect to the alkene complex **12-Cy**.

Observation of a σ-H_2 Complex and H/D Scrambling by [P_2Si]Rh. As noted above, calculations on the [$^{Me}P_2Si^{Me}$]Rh model system indicated that reaction of [$^{Cy}P_2Si^{Me}$]Rh (**^{Cy}1**) with H_2 may afford a σ-complex or a dihydride, since the isomers (dihydrogen complex **2** versus dihydrides **6** and **8**) differ computationally by <2 kcal/mol. Previous experiments with the related [$^{Cy}P_2Si^{OTf}$]Rh(nbd) precatalyst (nbd = norbornadiene) led to rearrangement to a more stable hydrosilyl complex, precluding identification of an η^2-H_2 or dihydride complex, so we were interested in using the methyl-substituted [$^{Cy}P_2Si^{Me}$]Rh to probe the interaction with hydrogen experimentally.

As expected, exposure of **^{Cy}1-nbd** to H_2 (1 atm) leads to immediate expulsion of nba, with formation of a single Rh product (**^{Cy}1-H_2**) characterized by a broad doublet ^{31}P NMR signal (δ 74.4 ppm, $^1J_{RhP}$ = 127 Hz) and a broad ^{1}H NMR signal (δ −2.38 ppm, $\Delta\nu_{1/2}$ = 50 Hz) consistent with an η^2-H_2 complex.[11] No coupling is observed between the H_2 ligand and either ^{31}P or ^{103}Rh. Upon cooling, the resonance broadens, and it is not resolvable below −15 °C. These spectral characteristics are quite similar to those reported by Milstein for the saturated [PCP]Rh(H_2) complex **A** (Chart 1),[12] which also did not exhibit any ^{1}H/^{31}P or ^{1}H/^{103}Rh coupling. In contrast, the pincer complexes **B** and **C** featuring a C_{aryl} donor show coupling of bound H_2 to rhodium, and **B** also shows well-resolved coupling to phosphorus.[13] The fact that no free H_2 is observed by NMR, combined with the broadness of the H_2 peak, may indicate fast exchange between free and bound H_2, including possibly hydrogen-atom scambling (*vide infra*). The weak binding of H_2 to **^{Cy}1** is further indicated by the instability of **^{Cy}1-H_2** under N_2 (presumably leading to a dinitrogen complex), which precludes its full characterization.

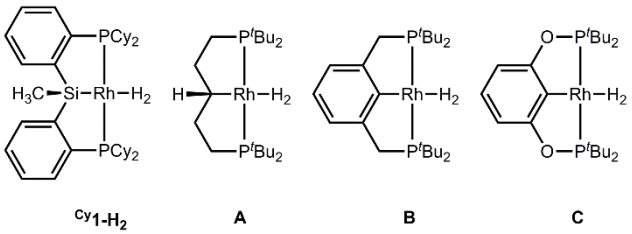

Chart 1. Pincer-type rhodium dihydrogen complexes

The formulation of **^{Cy}1-H_2** as a dihydrogen rather than dihydride complex is supported by T_1 measurements on the H_2 signal at 23 °C (45 ms) and −15 °C (27 ms), at least one order of magnitude shorter than would be expected for a classical dihydride complex.[11,14] We were not able to obtain T_1(min) because of the broadening of the signal at low temperature. Dihydrogen complexes are also frequently characterized by H/D coupling in the HD isotopologue. However, exposure of **^{Cy}1-nbd** to HD affords a product with a broad η^2-H_2 signal (integrated to one-half the value for **^{Cy}1-H_2**) with no resolvable HD coupling, a situation analogous to that reported by Weller and co-workers for Rh dihydrogen complexes supported by tricyclohexylphosphine ligands.[15]

Consistent with computations, **^{Cy}1-H_2** serves as an efficient catalyst for H/D scrambling between H_2 and D_2. For instance, under catalytically relevant conditions ([**^{Cy}1-nbd**] = 0.44 mM, 5.0 mL C_6H_6 solution, headspace volume = ca. 45 mL, P_{total} = 1 atm) but without alkene present, a 1:1 mixture of H_2/D_2 was 83% scrambled after 20 min (HD:H_2 ratio of 1.42). This finding suggests that **^{Cy}1-H_2** can easily access a dihydride form capable of H/D scrambling.

If an alkene adduct such as **1-nbe** is the resting state under catalytically relevant conditions, as suggested by computations (*vide supra*), then H/D scrambling should be inhibited in the presence of alkene. Indeed, when the H_2/D_2 scrambling experiment described above is conducted in the presence of 434 mM nbe (ca. 1000 equiv relative to **^{Cy}1-nbd**), the reaction is on the order of 15 times slower, giving only 11% scrambling after 20 min (HD:H_2 ratio of 0.12). Thus, although H/D scrambling among hydrogen gas molecules can occur under catalytically relevant conditions, it is severely inhibited, consistent with an olefin-bound catalyst resting state.

Although our calculations suggest that a dihydride isomer of **^{Cy}1-H_2** should lie at similar (or lower) energy, experimental evidence supports a σ-dihydrogen ground state with accessible dihydride that may participate in H/D scrambling. As noted above, computations suggest that an olefin-first mechanism is most important under our conditions, similar to what has been observed for classic cationic rhodium diphosphine catalysts.[16] Consequently, the dihydrogen complex **^{Cy}1-H_2** may lie off the primary catalytic pathway, though addition of nbe to this com-

plex would certainly be followed by facile H_2 scission and alkene insertion, consistent with related findings regarding insertion of CO_2 to Milstein's [PCP]RhH_2 complex **A**.[12,17]

Alkane Release at [P_2Si]Rh by Competitive σ-Bond Metathesis and Reductive Elimination. Having elucidated the nature of the interaction of [P_2Si]Rh with hydrogen, we turned our attention to the mechanism of alkane release. Most rhodium hydrogenation catalysts release hydrogenated product by R/H reductive elimination.[5a] However, a simple oxidative addition/reductive elimination pathway is not supported by our earlier observation of substantial nba-d_1 upon hydrogenation of nbe under H_2/D_2.

In order to understand the product distribution previously observed, we undertook the hydrogenation of nbe using HD to ensure an exact 1:1 H/D stoichiometry. If H/D scrambling is not faster than hydrogenation, then alkane release through reductive elimination (Path A in Figure 1) should generate only nba-d_1. Alternatively, if alkane release occurs only by σ-bond metathesis (Path B in Figure 1), then a statistical mixture of nba-d_0 (25%), -d_1 (50%), and -d_2 (25%) should be obtained in the absence of kinetic isotope effects (KIEs).

When nbe was hydrogenated using standard conditions (0.5 mol % catalyst) under HD (1 atm) at ambient temperature for 3 h, the hydrogenated product consisted of a 29:50:21 mixture of nba-d_0:d_1:d_2 (Table 1 and Figure S1). The presence of 50% d_1 product in the mixture suggests that alkane release occurs almost exclusively by σ-bond metathesis under these conditions. The modest excess of nba-d_0 versus -d_2 is likely due to one or more small isotope effects.

Since the ^{Cy}**1-nbd** precatalyst is capable of H/D scrambling, an alternate explanation for the above finding is that HD is scrambled to a statistical mixture of H_2, HD, and D_2 much more rapidly than hydrogenation occurs and reductive elimination is the preferred pathway for alkane release. Although some H/D scrambling undoubtedly occurs during the course of the reaction (*vide supra*), we disfavor this explanation based on the following observations:

(1) Sampling the headspace of a catalytic reaction under HD (1 atm) after 20 min reveals a 6:1 HD/H_2 ratio and a 28:50:22 distribution of nba-d_0:d_1:d_2 isotopomers, nearly identical to the relative amounts obtained from the 180-min reaction described above.

(2) Although H/D scrambling is efficient in the absence of alkene, it is significantly inhibited in the presence of alkene (*vide supra*).

Since σ-bond metathesis is a bimolecular process, it comes with a significant entropic penalty compared with unimolecular reductive elimination. Thus, any change in conditions that amplifies the entropic penalty (e.g., an increase in temperature or decrease in hydrogen pressure) should disfavor σ-bond metathesis. To test this proposal, hydrogenation of nbe was run at 50 °C under 1 atm and 0.25 atm of HD. As shown in Table 1, at elevated temperature nba-d_1 accounted for 55% (1 atm HD) and 60% (0.25 atm HD) of the observed products, consistent with an increasingly competitive reductive elimination pathway for alkane release. Thus, labelling experiments strongly support the computational prediction that bi- and unimolecular alkane release can be competitive processes. To the best of our knowledge, such a conclusion has not previously been demonstrated for any hydrogenation catalyst. Unfortunately, the presence of H/D scrambling precludes definitive assignments of energy differences for the various pathways. However, the product ratio at 50 °C and 0.25 atm HD suggests that σ-bond metathesis is approximately 4-fold faster than reductive elimination under these conditions ($\Delta\Delta G^{\ddagger} < 1$ kcal/mol). These findings provide a close match with computations (*vide supra*).

The reactions under various conditions also highlight the changing isotope effect as temperature is increased. The nba-d_0/nba-d_2 ratio should be equal to the KIE or product of isotope effects for relevant C–H/C–D bond-forming steps. The nba-d_0/nba-d_2 ratio at 25 °C (1.36) is slightly higher than observed at 50 °C (1.20), consistent with the expectation for a decreased isotope effect at increased temperature. However, the ratio is independent of HD concentration at a given temperature (entries 2 and 3 in Table 1), as expected.

Table 1. Norbornene hydrogenation under HD[a]

Entry	Conditions		norbornane isotopomers (%)		
	T (°C)	P_{HD} (atm)	d_0	d_1	d_2
1	25	1	28.9	49.9	21.2
2	50	1	24.4	55.2	20.3
3	50	0.25	21.5	60.5	18.0

[a] [nbe] = 76 mM, [Rh] = 0.38 mM in 5 mL C_6H_6 under 45 mL HD at specified pressure.

Discussion. Based on the combined findings presented above, we propose a modestly revised mechanism for alkene hydrogenation at [P_2Si]Rh (Figure 8). First, the catalyst ^{Cy}**1** interacts with H_2 to make a dihydrogen σ-complex, not a dihydride. However, an energetically accessible dihydride isomer enables efficient H/D scrambling by ^{Cy}**1-H$_2$**. Computations show that H_2 oxidative addition occurs after addition of alkene; this may come about through association of nbe to the dihydrogen complex ^{Cy}**1-H$_2$** or through association of H_2 to the norbornene adduct ^{Cy}**1-nbe**. Under the conditions examined, calculations suggest that the olefin-first route predominates (bottom path in Figure 8), and both experimental and computational findings support an olefin-bound resting state for the catalyst. However, the fact that catalysis is quite slow in spite of low (17 kcal/mol) calculated barriers may support a lower-energy, off-cycle resting state such as the bis(alkene) complex [P_2Si]Rh(nbe)$_2$.

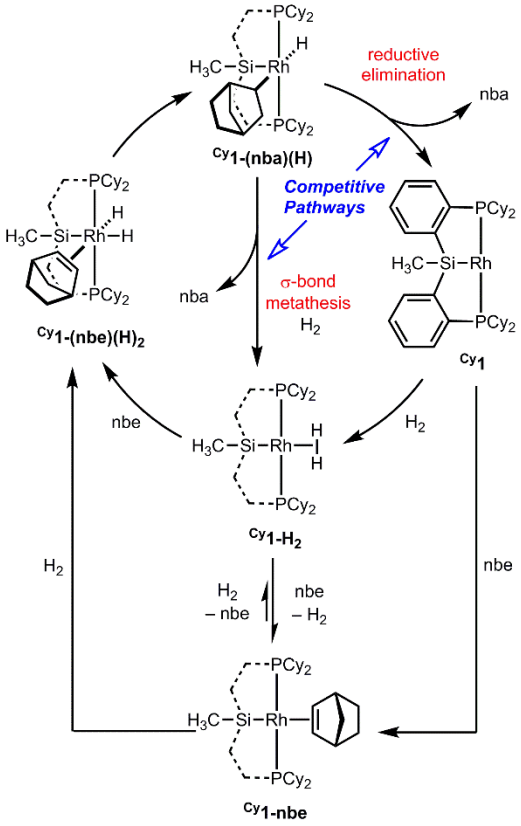

Figure 8. Revised mechanism for nbe hydrogenation by [^{Cy}P$_2$Si^{Me}]Rh (**^{Cy}1**).

Our findings regarding interaction of **^{Cy}1** with H_2 suggest approximately isoenergetic Rh(I)/Rh(III) and would seem to indicate that reductive elimination to release alkane and regenerate **^{Cy}1** should be facile. However, our combined experimental and computational approach has also shown that alkane release occurs by *competitive* reductive elimination and σ-bond metathesis pathways, with σ-bond metathesis predominating under all conditions examined.

The degree to which σ-bond metathesis effectively competes with reductive elimination is unusual for rhodium-based hydrogenation systems (especially one that does not readily undergo H_2 oxidative addition) and merits further discussion. The [P_2Si] pincer-type ligands described herein contain an exceptionally strongly *trans*-influencing silyl donor (Si > H > C).[10a,18] The positioning of the Si donor as a central element in the pincer scaffold tends favor 5-coordinate complexes with square-pyramidal geometry and an empty coordination site *trans* to Si. Consequently, the norbornyl hydride intermediate (top structure in Figure 7) that forms *en route* to the alkane features *trans*-disposed alkyl and hydride ligands. Since reductive elimination requires a *cis* arrangement of eliminating ligands, this feature results in a considerable rearrangement penalty prior to alkane release. Furthermore, the presence of a vacant coordination site *trans* to Si and *cis* to the norbornyl ligand in the 16-electron norbornyl hydride intermediate provides an appropriate arrangement for σ-bond metathesis.

The above findings show that our system is in some sense uniquely constructed to encourage alkane release by σ-bond metathesis at Rh. These findings also explain why catalysis is slow: the same features that engender an unusual set of competitive reactivity slow catalysis, since intermediates with *trans*-disposed alkyl and hydride ligands are also energetically unfavorable.

CONCLUSIONS

In this paper, we have taken a combined experimental and computational approach to elucidating key aspects of the mechanism of alkene hydrogenation by pincer-type [P_2Si]Rh complexes. Computational predictions have played a particularly important role in illuminating a set of competitive mechanisms for alkane release in the hydrogenation process, showing that bimolecular (σ-bond metathesis) and unimolecular (reductive elimination) processes may be energetically similar. This prediction has been confirmed by hydrogenation of nbe with HD at different temperatures and HD pressures.

Overall, our findings show both the unique challenges and opportunities afforded by pincer-type complexes featuring a strongly *trans*-influencing silyl donor, supplementing previous work on pincer-type [P_2Si] systems.[19] Though it is tempting to assume that competitive σ-bond metathesis and reductive elimination are not generally operative in rhodium-catalyzed hydrogenation, our findings suggest that σ-bond metathesis should be considered as a mechanistic possibility, particularly in reactions run under high H_2 pressure. The results presented herein also draw attention to the unexpected consequences that can result from apparently subtle changes to the ligand backbone.

EXPERIMENTAL SECTION

General Considerations. All manipulations were carried out under a dinitrogen atmosphere in an MBraun Unilab 2000 glove box or on a Schlenk line using standard techniques. Routine solvents were deoxygenated and dried using a Glass Contour Solvent Purification System, except for anhydrous benzene and pentane, which were purchased as anhydrous and used as received. NMR solvents were dried over Na/Ph_2CO and vacuum-transferred prior to use. NMR spectra were recorded on a Bruker Avance III HD 400 High Performance Digital NMR spectrometer. ^{1}H chemical shifts were referenced to residual solvent and ^{31}P NMR chemical shifts are reported relative to an external standard of 85% H_3PO_4.

Preparation of [^{Cy}P$_2$Si^{Me}]Rh(nbd) (^{Cy}1-nbd). [^{Cy}P$_2$Si^{Me}]Rh(H)(Cl)[20] (54.3 mg, 0.0746 mmol) and excess norbornadiene (7 drops, ca. 100 mg) were dissolved in benzene (5 mL). A solution of lithium triethylborohydride (1.0 M in THF, 75 µL, 0.075 mmol) was diluted in benzene (1 mL) and added dropwise to the Rh solution with stirring. After 10 min, the mixture was heated in a sealed vial at 80 °C for 45 min. The resulting mixture was filtered to remove LiCl, frozen, and lyophilized to give a **^{Cy}1-nbd** as a yellow-brown powder. The product was further purified by crystallization via slow evaporation of pentane from a concentrated solution at −35 °C over a period of 24 h, affording pure **^{Cy}1-nbd** as yellow crystals (48.9 mg, 84%). Spectroscopic data matched those from our previous report.[7]

[^{Cy}P$_2$Si^{Me}]Rh(H$_2$) (^{Cy}1-H$_2$). In a Wilmad LPV NMR tube, a solution of **^{Cy}1-nbd** (ca. 8 mg) in C_6D_6 (0.7 mL) was frozen and the headspace evacuated and backfilled with hydrogen (1 atm). Upon thawing, the tube was inverted several times to ensure efficient H_2 mixing, and the solution color changed from yellow to dark red, then back to yellow. ^{31}P NMR spectroscopy indicated complete reaction after <5 min, though a small amount of unidentified byproduct (3–7% by ^{31}P NMR) was routinely also observed. The instability of **^{Cy}1-H$_2$** in the absence of H_2 atmosphere precluded further purification or analysis by techniques other than NMR spectroscopy. ^{1}H NMR (400 MHz, C_6D_6): δ 8.03 (d, J = 7.2 Hz, 2H), 7.48 (d, J = 7.4 Hz, 2H), 7.26 (t, J = 7.2 Hz, 2H), 7.16 (t, J = 7.2 Hz, 2H, *overalapping with C_6D_5H*), 2.06 (m, 2H), 1.90 (m, 2H), 1.74–1.06 (m, 40H, *overlapping with free nba*), 1.03 (s, 3H, Si–C*H*$_3$), –2.70 (br s, 2H, Rh–*H*$_2$). ^{31}P{^{1}H} NMR (162 MHz, C_6D_6): δ 74.3 (br d, $^1J_{RhP}$ = 128 Hz). *Note:* **^{Cy}1-HD** was made by the same procedure and proved spectroscopically identical except that the integration of the bound HD signal was equivalent to only one proton.

Hydrogenation of nbe under HD. Stock solutions of ^{Cy}**1-nbd** (1.85 mL, 0.0051 mM in C_6H_6) and nbe (1.80 mL, 1.06 mM in C_6H_6) were combined and diluted to 5.0 mL in a volumetric flask. The mixture was transferred to a 50-mL pressure tube, the solution was subjected to three freeze–pump–thaw cycles, and the headspace backfilled with HD (1.0 atm or 0.25 atm). The mixtures were warmed to 25 °C or 50 °C and allowed to react with stirring for 3 h. The resulting solutions were filtered through a plug of alumina and analyzed by GC-MS. The distribution of nba isotopomers was determined as described in the Supporting Information.

H_2/D_2 scrambling analysis in the presence and absence of nbe. A 10.-mL stock solution containing ^{Cy}**1-nbd** (0.44 mM) in benzene was split into two 50-mL pressure tubes and norbornene (204 mg, 2.17 mmol) was added to one to give a final concentration of 434 mM. Both solutions were subjected to a freeze–pump–thaw cycle and the headspaces backfilled with 1:1 H_2/D_2 by first adding H_2 (0.5 atm) then opening the flasks to D_2 (1 atm). The solutions were quickly warmed to room temperature in a water bath and allowed to react with vigorous stirring for 20 min. The headspaces (10 mL each) were sampled with a gastight syringe and bubbled through C_6D_6 in a Wilmad LPV NMR tube. The resulting HD:H_2 ratio was determined by ^{1}H NMR spectroscopy by integrations of the H_2 (δ 4.47 (s)) and HD (δ 4.44 (t (1:1:1), $^1J_{HD}$ = 42.7 Hz) signals.

ASSOCIATED CONTENT

Supporting Information

The Supporting Information is available free of charge on the ACS Publications website.

NMR spectra for ^{Cy}**1-H_2** and H_2/D_2 scrambling; mass spectra for nbe hydrogenation under HD and detailed method for assigning nba isotopomer distribution; computational details, energies of all computed structures, a comparison of other functionals and treatments of entropy, higher-energy isomers not shown in the main text, and IRC data (PDF)

Coordinates of all intermediates and transition states (XYZ)

AUTHOR INFORMATION

Corresponding Author

* E-mail: mwhited@carleton.edu
* E-mail: taylorb@up.edu

ORCID

Matthew T. Whited: 0000-0002-1193-9078
Buck L. H. Taylor: 0000-0002-6586-3865

Author Contributions

§ These authors contributed equally.

Notes

The authors declare no competing financial interests.

ACKNOWLEDGMENT

This material is based upon work supported by a CAREER award from the National Science Foundation (CHE-1552591 to M.T.W.). NMR spectroscopy was enabled by NSF-MRI Award No. 1428752, "MRI: Acquisition of a 400 MHz NMR Spectrometer to Support Research and Undergraduate Research Training at Carleton College and St. Olaf College". M.T.W. is a Henry Dreyfus Teacher-Scholar. Computational resources were provided by an NSF-MRI award (CHE-1039925) through the Midwest Undergraduate Computational Chemistry Consortium (MU3C), as well as the Extreme Science and Engineering Discovery Environment (XSEDE), which is supported by NSF award ACI-1548562. Professor David Alberg is acknowledged for helpful suggestions regarding headspace analysis of hydrogenation reactions.

REFERENCES

(1) (a) Halpern, J.; Okamoto, T.; Zakhariev, A. "Mechanism of Chlorotris(triphenylphosphine)rhodium(I)-Catalyzed Hydrogenation of Alkenes - Reaction of Chlorodihydridotris(triphenylphosphine)rhodium(III) with Cyclohexene" *J. Molec. Catal.* **1977**, *2*, 65-68. (b) *The Handbook of Homogeneous Hydrogenation*; de Vries, J. G.; Elsevier, C. J., Eds.; WILEY-VCH: Weinheim, 2007. (c) Hartwig, J. F. In *Organotransition Metal Chemistry: From Bonding to Catalysis*; University Science Books: Sausalito, CA, 2010, p 575-665. (d) Gridnev, I. D.; Higashi, N.; Asakura, K.; Imamoto, T. "Mechanism of Asymmetric Hydrogenation Catalyzed by a Rhodium Complex of (*S*,*S*)-1,2-Bis(tert-butylmethylphosphino)ethane. Dihydride Mechanism of Asymmetric Hydrogenation" *J. Am. Chem. Soc.* **2000**, *122*, 7183-7194. (e) Felgdus, S.; Landis, C. R. In *Computational Modeling of Homogeneous Catalysis*; Maseras, F., Lledos, A., Eds.; Kluwer: Dordrecht, 2002; Vol. 25, p 107-135. (f) Rohmann, K.; Holscher, M.; Leitner, W. "Can Contemporary Density Functional Theory Predict Energy Spans in Molecular Catalysis Accurately Enough To Be Applicable for in Silico Catalyst Design? A Computational/Experimental Case Study for the Ruthenium-Catalyzed Hydrogenation of Olefins" *J. Am. Chem. Soc.* **2016**, *138*, 433-443.

(2) (a) Waterman, R. "σ-Bond Metathesis: A 30-Year Retrospective" *Organometallics* **2013**, *32*, 7249-7263. (b) Coperet, C. In *The Handbook of Homogeneous Hydrogenation*; De Vries, J. G., Elsevier, C. J., Eds.; WILEY-VCH: Weinheim, 2007; Vol. 1, p 111-151.

(3) Morris, R. H. In *The Handbook of Homogeneous Hydrogenation*; De Vries, J. G., Elsevier, C. J., Eds.; WILEY-VCH: Weinheim, 2007; Vol. 1, p 45-70.

(4) Perutz, R. N.; Sabo-Etienne, S. "The σ-CAM Mechanism: σ Complexes as the Basis of σ-Bond Metathesis at Late-Transition-Metal Centers" *Angew. Chem., Int. Ed.* **2007**, *46*, 2578-2592.

(5) (a) Oro, L. A.; Carmona, D. In *The Handbook of Homogeneous Hydrogenation*; De Vries, J. G., Elsevier, C. J., Eds.; WILEY-VCH: Weinheim, 2007; Vol. 1, p 3-30. (b) Crabtree, R. H. In *The Handbook of Homogeneous Hydrogenation*; De Vries, J. G., Elsevier, C. J., Eds.; WILEY-VCH: Weinheim, 2007; Vol. 1, p 31-44.

(6) (a) Whited, M. T.; Deetz, A. M.; Boerma, J. W.; DeRosha, D. E.; Janzen, D. E. "Formation of Chlorosilyl Pincer-Type Rhodium Complexes by Multiple Si-H Activations of Bis(phosphine)/Dihydrosilyl Ligands" *Organometallics* **2014**, *33*, 5070-5073. (b) Whited, M. T. "Metal-Ligand Multiple Bonds as Frustrated Lewis Pairs for C-H Functionalization" *Beilstein J. Org. Chem.* **2012**, *8*, 1554-1563. (c) Whited, M. T.; Qiu, L.; Kosanovich, A. J.; Janzen, D. E. "Chalcogen Extrusion from Heteroallenes and Carbon Monoxide by a Three-Coordinate Rh(I) Disilylamide" *Inorg. Chem.* **2015**, *54*, 3670-3679. (d) Whited, M. T.; Kosanovich, A. J.; Janzen, D. E. "Synthesis and Reactivity of Three-Coordinate (dtbpe)Rh Silylamides: CO_2 Bond Cleavage by a Rhodium(I) Disilylamide" *Organometallics* **2014**, *33*, 1416-1422.

(7) Whited, M. T.; Deetz, A. M.; Donnell, T. M.; Janzen, D. E. "Examining the Role of Rh/Si Cooperation in Alkene Hydrogenation by a Pincer-Type [P_2Si]Rh Complex" *Dalton Trans.* **2016**, *45*, 9758-9761.

(8) Frisch, M. J.; Trucks, G. W.; Schlegel, H. B.; Scuseria, G. E.; Robb, M. A.; Cheeseman, J. R.; Scalmani, G.; Barone, V.; Mennucci, B.; Petersson, G. A.; Nakatsuji, H.; Caricato, M.; Li, X.; Hratchian, H. P.; Izmaylov, A. F.; Bloino, J.; Zheng, G.; Sonnenberg, J. L.; Hada, M.; Ehara, M.; Toyota, K.; Fukuda, R.; Hasegawa, J.; Ishida, M.; Nakajima, T.; Honda, Y.; Kitao, O.; Nakai, H.; Vreven, T.; Montgomery Jr., J. A.; Peralta, J. E.; Ogliaro, F.; Bearpark, M. J.; Heyd, J.; Brothers, E. N.; Kudin, K. N.; Staroverov, V. N.; Kobayashi, R.; Normand, J.; Raghavachari, K.; Rendell, A. P.; Burant, J. C.; Iyengar, S. S.; Tomasi, J.; Cossi, M.; Rega, N.; Millam, N. J.; Klene, M.; Knox, J. E.; Cross, J. B.; Bakken, V.; Adamo, C.; Jaramillo, J.; Gomperts, R.; Stratmann, R.

E.; Yazyev, O.; Austin, A. J.; Cammi, R.; Pomelli, C.; Ochterski, J. W.; Martin, R. L.; Morokuma, K.; Zakrzewski, V. G.; Voth, G. A.; Salvador, P.; Dannenberg, J. J.; Dapprich, S.; Daniels, A. D.; Farkas, Ö.; Foresman, J. B.; Ortiz, J. V.; Cioslowski, J.; Fox, D. J. *Gaussian 09*, Gaussian, Inc.: Wallingford, CT, USA, 2009.

(9) Corey, J. Y. "Reactions of Hydrosilanes with Transition Metal Complexes" *Chem. Rev.* **2016**, *116*, 11291-11435.

(10) (a) Aizenberg, M.; Milstein, D. "Facial (methyl)(hydrido)(silyl) Complexes of Iridium: Synthesis, X-ray Structures, and Reductive Elimination Reactions. Facile Formation of Silametalacycles by Metalation of Silyl Ligands" *J. Am. Chem. Soc.* **1995**, *117*, 6456-6464. (b) Zhu, J.; Lin, Z. Y.; Marder, T. B. "Trans influence of boryl ligands and comparison with C, Si, and Sn ligands" *Inorg. Chem.* **2005**, *44*, 9384-9390.

(11) Kubas, G. J. *Metal Dihydrogen and σ-Bond Complexes*; Springer: New York, 2001.

(12) Vigalok, A.; BenDavid, Y.; Milstein, D. "Complexation of N_2, H_2, CO_2, and Ethylene to a T-Shaped Rhodium(I) Core" *Organometallics* **1996**, *15*, 1839-1844.

(13) (a) Nemeh, S.; Jensen, C.; Binamirasoriaga, E.; Kaska, W. C. "Interaction of {2,6-Bis[(di-tert-butylphosphino)methyl]phenyl}rhodium(I) with Hydrocarbons. X-ray Molecular Structure of {2,6-Bis[(di-tert-butylphosphino)methyl]phenyl}chlorohydridorhodium(III)" *Organometallics* **1983**, *2*, 1442-1447. (b) Xu, W. W.; Rosini, G. P.; Gupta, M.; Jensen, C. M.; Kaska, W. C.; KroghJespersen, K.; Goldman, A. S. "Thermochemical Alkane Dehydrogenation Catalyzed in Solution without the use of a Hydrogen Acceptor" *Chem. Commun.* **1997**, 2273-2274. (c) Findlater, M.; Schultz, K. M.; Bernskoetter, W. H.; Cartwright-Sykes, A.; Heinekey, D. M.; Brookhart, M. "Dihydrogen Complexes of Iridium and Rhodium" *Inorg. Chem.* **2012**, *51*, 4672-4678.

(14) Crabtree, R. H. "Dihydrogen Complexation" *Chem. Rev.* **2016**, *116*, 8750-8769.

(15) Ingleson, M. J.; Brayshaw, S. K.; Mahon, M. F.; Ruggiero, G. D.; Weller, A. S. "Dihydrogen Complexes of Rhodium: $[RhH_2(H_2)_x(PR_3)_2]^+$ (R = Cy, ^{i}Pr; x = 1, 2)" *Inorg. Chem.* **2005**, *44*, 3162-3171.

(16) (a) Halpern, J.; Riley, D. P.; Chan, A. S. C.; Pluth, J. J. "Novel Coordination Chemistry and Catalytic Properties of Cationic 1,2-Bis(diphenylphosphino)ethanerhodium(I) Complexes" *J. Am. Chem. Soc.* **1977**, *99*, 8055-8057. (b) Chan, A. S. C.; Halpern, J. "Interception and Characterization of a Hydridoalkylrhodium Intermediate in a Homogeneous Catalytic Hydrogenation Reaction" *J. Am. Chem. Soc.* **1980**, *102*, 838-840.

(17) Huang, K. W.; Han, J. H.; Musgrave, C. B.; Fujita, E. "Carbon Dioxide Reduction by Pincer Rhodium η^2-Dihydrogen Complexes: Hydrogen-Binding Modes and Mechanistic Studies by Density Functional Theory Calculations" *Organometallics* **2007**, *26*, 508-513.

(18) Spessard, G. O.; Miessler, G. L. *Organometallic Chemistry*; 3rd ed.; Oxford University Press: New York, 2016.

(19) (a) Morgan, E.; MacLean, D. F.; McDonald, R.; Turculet, L. "Rhodium and Iridium Amido Complexes Supported by Silyl Pincer Ligation: Ammonia N-H Bond Activation by a PSiP Ir Complex" *J. Am. Chem. Soc.* **2009**, *131*, 14234-+. (b) MacInnis, M. C.; MacLean, D. F.; Lundgren, R. J.; McDonald, R.; Turculet, L. "Synthesis and Reactivity of Platinum Group Metal Complexes Featuring the New Pincer-like Bis(phosphino)silyl Ligand $[\kappa^3\text{-}(2\text{-}Ph_2PC_6H_4)_2SiMe]^-$ ([PSiP]): Application in the Ruthenium-Mediated Transfer Hydrogenation of Ketones" *Organometallics* **2007**, *26*, 6522-6525. (c) Takaya, J.; Iwasawa, N. "Hydrocarboxylation of Allenes with CO_2 Catalyzed by Silyl Pincer-Type Palladium Complex" *J. Am. Chem. Soc.* **2008**, *130*, 15254-15255. (d) Takaya, J.; Kirai, N.; Iwasawa, N. "Efficient Synthesis of Diborylalkenes from Alkenes and Diboron by a New PSiP-Pincer Palladium-Catalyzed Dehydrogenative Borylation" *J. Am. Chem. Soc.* **2011**, *133*, 12980-12983. (e) Suh, H. W.; Guard, L. M.; Hazari, N. "A Mechanistic Study of Allene Carboxylation with CO_2 Resulting in the Development of a Pd(II) Pincer Complex for the Catalytic Hydroboration of CO_2" *Chem. Sci.* **2014**, *5*, 3859-3872. (f) Simon, M.; Breher, F. "Multidentate Silyl Ligands in Transition Metal Chemistry" *Dalton Trans.* **2017**, *46*, 7976-7997.

(20) MacLean, D. F.; McDonald, R.; Ferguson, M. J.; Caddell, A. J.; Turculet, L. "Room Temperature Benzene C-H Activation by a New [PSiP]Ir Pincer Complex" *Chem. Commun.* **2008**, 5146-5148.